ynthetic Aperture Radar

Classifying Open-Air Radar Signals using a Simulation-Trained Machine Learning Network

THESIS

Matthew M. ROfrano, B.S.E.E., Captain, USAF

AFIT-ENG-MS-20-M-XXX

DEPARTMENT OF THE AIR FORCE
AIR UNIVERSITY

AIR FORCE INSTITUTE OF TECHNOLOGY

Wright-Patterson Air Force Base, Ohio

AFIT-ENG-MS-20-M-XXX

Classifying Open-Air Radar Signals using a Simulation-Trained Machine Learning Network

THESIS

Presented to the Faculty
Department of Electrical and Computer Engineering
Graduate School of Engineering and Management
Air Force Institute of Technology
Air University
Air Education and Training Command
in Partial Fulfillment of the Requirements for the
Degree of Master of Science in Electrical Engineering

Matthew M. ROfrano, B.S.E.E., B.S.E.E.
Captain, USAF

March XX, 2023

AFIT-ENG-MS-20-M-XXX

Classifying Open-Air Radar Signals using a Simulation-Trained Machine Learning Network

THESIS

Matthew M. ROfrano, B.S.E.E., B.S.E.E.
Captain, USAF

Committee Membership:

Robert F. Mills, Ph.D
Chair

Charles XX. Macon,, Ph.D
Member

DUNNO-SOME LO DUDE,, Ph.D
Member

AFIT-ENG-MS-20-M-XXX

Abstract

The proliferation of Low Observable (LO) aircraft and Electronic Counter Measure (ECM) will complicate the ability of radar systems to accurately identify adversary aircraft. Advances in machine learning are enabling sensors to better identify patterns in signal data, and make more informed decisions. This paper investigates the classification accuracy of XX Machine Learning (ML) models as compared to a traditional matched filter receiver. The ML models have been pretrained using a model based approach. Simulated Radar Cross Section (RCS) data for XX targets was created using Altair's CADFeko Electromagnetic Simulation (ESIM) software. Models used for the ESIM are simplified 3D CAD models based on physical targets. Simulation data was forked into two training sets: a feature-based set that feeds the raw RCS data to the ML model; and a probability based set that creates causal PDFs using the mean and variance over frequency. The trained models are tested using measurement data collected in Air Force Institute of Technology (AFIT)'s indoor compact radar range. Classification accuracy for each ML model will be reported in a confusion matrix along with a corresponding F-1 number. Accuracy metrics are used to create a Radar Operating Curve (ROC) plot for each target.

Table of Contents

List of Figures

List of Tables

Classifying Open-Air Radar Signals using a Simulation-Trained Machine Learning Network

I. Introduction

1.1 Problem Background

The Department of Defense recognizes the critical importance of the Electromagnetic spectrum – It is a battleground, inseperable from and with equivelent importance to the classical settings of war [1].

1.1.1 Subsection Title Here

Subsection text here

1.2 Research Objectives

Research objectives here.

1.3 Document Overview

Reference chapters and sections like Chapter I or Chapter II.

II. Background and Literature Review

Background on the S (SAR) Automatic Target Recognition (ATR) communities investigations regarding sensor model training approach is provided. A taxonomy of three training styles is reviewed, and a fourth is proposed.

2.1 Electromagnetic Waves

- Need to reference the Kong text her to make sure I get this right - The behaviour of electromagnetic waves is driven by boundary conditions. A boundary is considered a region over which material properties change. Principally, the electromagnetic propoerties of permittivity, ϵ, and permiability, μ. - Explain why these matter, and how they are related via snells law. Permitivitty, given in "PROVIDE UNITS", . Consider the interface between air and a metal sheet: the constituant parameters of air is a boundary. EM wave energy is conservedAs an EM wave transits from one material to

2.2 Radar

The transit speed, and reflective interaction with metallic targets make electromagnetic waves an ideal tool for long distance target detection. The first radio detection and ranging (Radar) device was patented by German inventor Christian Hülsmeyer. Serving as a means to help ships avoid collision in heavy fog, radar showed impressive all weather, long distance performance. This concept was expanded on by a British meteorologist named Robert Watson-Watt. Watt measured the electromagnetic radiation from lighting bursts using an oscilloscope to track storms. Watt's innovation was using an oscilloscope to display the signals, allowing for better fidelity than the simple Hülsmeyer detector. The British Air Ministry, sensing an impending war with Germany quickly pressed this new capability into military service. In November 1934 the Committee for the Scientific Survey of Air Defense convened, chaired by Sir Henry Tizard. Watt and his assistant Arnold 'Skip' Wilson proposed a radar system that could not only detect enemy aircraft, but could determine their range as well. The first operational pulse radar utilized a $25\mu s$ pulse, pulse reputation interval of $25Hz$, peak power of $1kW$, and operating frequency of $6MHz$. This system detected a Supermarine Scapa flying boat at a distance of 17 miles on 17 June 1935, ushering in the era of air defense radars in modern warfare [2].

2.2.1 The Radar Equation

Generally, radar can be calculated using equation 1, the radar equation (RE) [3].

$$P_r = \frac{P_t}{4\pi R^2} G_t \cdot \frac{\sigma(\theta, \phi)}{4\pi R^2} \cdot \frac{G_r \lambda^2}{4\pi} \tag{1}$$

The RE can be broken into three terms representing the transmitter ($\frac{P_t}{4\pi R^2} G_t$); target ($\frac{\sigma}{4\pi R^2}$); and receiver ($\frac{G_r \lambda^2}{4\pi}$). Transmitter power is given as P_t; 4π evolves from the solution of an electromagnetic wave launched from a dipole antenna using Green's Functions(CITE KONG AND BE SURE TO SHOW THIS), with R^2 representing the distance from the transmitter to the target. Together, $\frac{P_t}{4\pi R^2}$ model the surface of an expanding sphere, over which the transmitters power is spread which is referred to as *isotropic* radiation. Radar detection range is dependent on transmission power. To maximize the detection range for a fixed input power, designers concentrate transmitted power into desired patterns by leveraging antenna designs. Electromagnetic energy will be transmitted from an antenna in a directional pattern driven by the physical construction of the antenna, referred to as the *directionality,* D of the antenna. The term G_t in the RRE is the gain of the radar, which subtracts power loss from the amplifier to the feed port of the antenna from the directionality [3].

The target term can be thought of as the "unpowered transmission" of an echo signal. The radiation surface of the echoed signal is modeled by the familiar $4\pi R^2$, however now the transmission power and gain variables have been replaced by the targets radar cross section, σ (RCS). A targets RCS encodes the reflectivity of the target for all incident angles θ and ϕ. The RCS term is empirically derived and is typically derived using a combination of indoor and outdoor range measurements and electromagnetic simulation software. Target RCS will be discussed in detail in a later section.

The third term models the radar's effective aperture, or the cross-sectional area of the antenna that can successfully capture incident radiation. The receivers gain is given as G_r, and the incident radiation's wavelength given as λ.

2.2.2 Signal to Noise Performance

Radars must contend with noise from several sources. Cosmic noise emanating from space is significant, but only below 1 GHz. Solar noise is largely mitigated by directional antennas, and only becomes a factor when the antenna is pointed directly at the sun. The ground produces noise similar to sun, though less intense and is also mitigated by directional antennas [3]. The two primary sources of noise that radar systems must contend with are *thermal* and *jamming* noise. Thermal noise is created by the random fluctuations of electrical charges [4]. Thermal noise is an omnipresent source with a power given by equation 2[5][6].

$$P_n = k_B T_S B = k_B T_0 F B \tag{2}$$

Where k_B is the Boltzmann Constant [1], T_S is the system temperature, B is the instantaneous receiver bandwidth in Hz, T_0 is the standard temperature [2], and F is

[1] $1.38 \times 10^{-23} W \cdot s/K$
[2] $T_0 = 290K$

the noise figure of the receiver subsystem. System bandwidth is typically driven by the signal the radar emits, and cannot be made arbitrarily small. A radar pulse of length τ will require a bandwidth of $B = 1/\tau$ [5]. Thermal noise is modelled as a zero-mean, gaussian process (I think the nyquist paper says this? note really sure if Im reading it right though.). Thermal noise sets the *noise floor* of the radar system. Signals with a power level below the noise floor will be indistinguishable from noise. A hypothetical system with a noise figure of 1.2, and bandwidth of 1 MHz will have a noise floor of $-112.8[dB_m]$.

Typically, the RE is cast in terms of range as shown in equation 3, the radar range equation (RRE). [3]. The RE solves for a an expected power level, where the RRE solves for an expected target range.

$$SNR_0 = \frac{P_t G_t G_r \lambda^2 \sigma}{(4\pi)^3 R^4 k_B T_0 F B} \tag{3}$$

The received power in equation 1 is divided by the thermal noise from equation **??** to produce a single-pulse signal to noise ratio, SNR_0.

Modern radar designs integrate multiple radar pulses to improve the SNR of the system. Integration leverages the zero-mean nature of thermal noise: continuously adding random zero mean noise will eventually reduce it to zero (Need a good citation for this process that isnt just POMR). The SNR improvement depends on the type of integration employed: coherent integration (in which phase information is preserved) applies a factor of n_p, and a factor of $\sqrt{n_p}$ for incoherent integration.

[3] This equation assumes a mono-static system: the radar uses a single antenna for both transmit and receive.

2.3 Radar Cross Section

2.4 Machine Learning Models

Discuss: - SVM - Random Forest - Neural Networks - K-nearest neighbor (K-NN) - What else?

2.5 Target Recognition

Training radars to automatically recognize targets using model data has been extensively studies by the SAR-ATR community [7]. A 2016 study proposes three taxonomy to describe the training methods employed when developing a sensor: 1. Feature based training; 2. Semi-model based training; 3. Model based training.

2.5.1 Feature-Based Training

The most common approach across SAR-ATR literature, feature based training utilizes either raw or template image-data to train a sensor. This approach assumes the features of an image are separable across classes [7].

While deeply researched and computationally accessible, feature based training suffers from statistical classification breakdown, and pattern recognition problems [7]. Further, the feature based approach requires preliminary training data, which could become untenable when employed for military's employment. Governments and their militaries got to great lengths to set a standard for how national secrets are classified and controlled [8][9], making it unreasonable to expect to have access to data that has been collected on adversary materiel. Using this method to train a traditionally radar system for target recognitions would be especially challenging: a target recognition algorithm would need calibrated data captured over a targets entire angular space azimuth to create a useful training set.

Model based training utilizes ESIM software to produce training data. In its simplest conception, the "model based" approach can be thought of as a data generator for a feature based training regime. That is, a system can be trained to identify features using modeled data, providing a sensor with otherwise inaccessible data.

Alternately, generated models can be processed to provide the sensor with a more "bottom-up" training approach. The "bottom-up" concept was developed and implemented by Robert A. Brooks at M.I.T. for the ACRONYMN target recognition system [10][11]. Simulation results are processed to produce scattering-center templates that are used to train the sensor. This method shifts the focus of training away from what the target looks in a specific limited instance, to something more representative of *how* the target *may* look.

Semi-model based training borrows from both feature and model based training: the limited feature based data set is processed to produce scattering center models. This method seeks the best of both world: robust, "behavior" based models that are built with limited, but readily available data sets.

The similarity in operation of a SAR and traditional radar make these taxonomy applicable to target identification in air defense. A feature based approach would utilize measured radar cross section data to train a sensor. A model-based approach utilizes utilize simulation results that have been calculate for a 3D model that is representative of the desired target. And a semi-model based approach would leverage measurement data to create a more robust, probabilistic model that could be used to train a sensor.

Machine learning models require data. The purpose of a machine learning model is to ingest data, and produce a desirable output. For this paper, that output is a classification. Classification models are typically built using a supervised training process, wherein an ML model is trained to make a classification using labeled data.

Labeled data is a data set where the input data is explicitly tethered to a unique classification label.

Text description here, can reference other Chapters or Sections, like Chapter I or Figure 1.

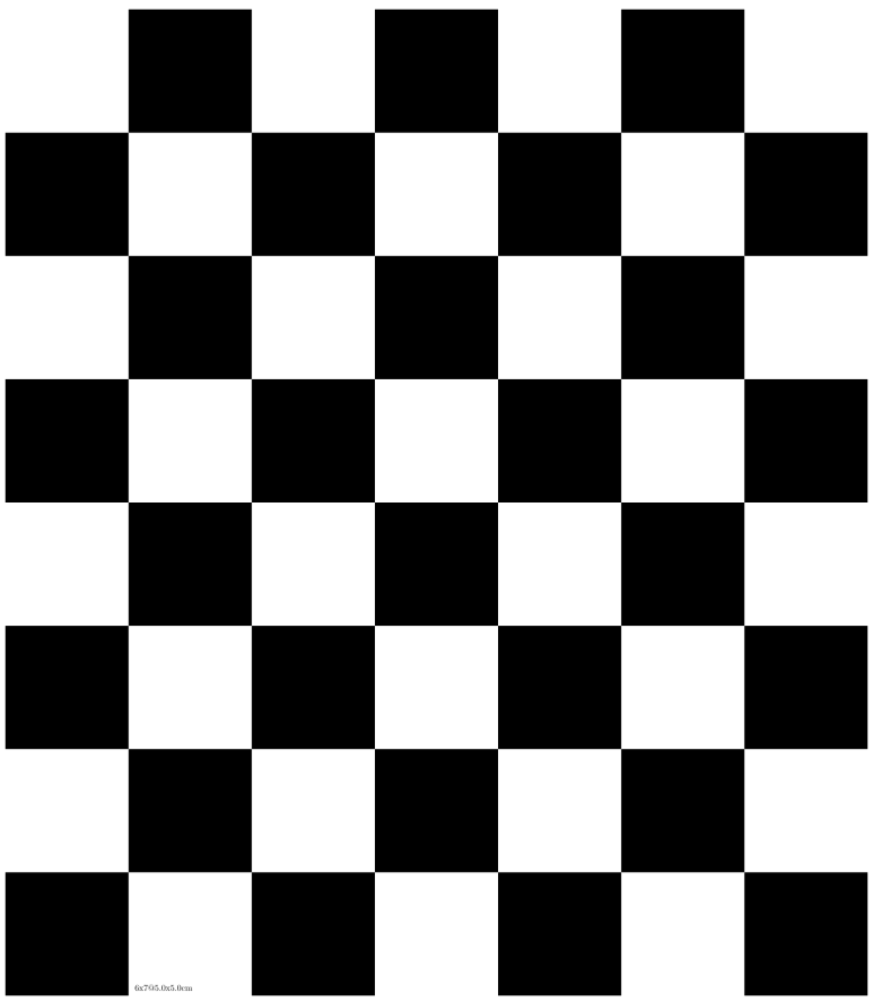

Figure 1: Title shown in text here: short paragraph description of picture here

2.6 Radar Cross Section

An RCS encodes the expected angular response of a target in the presence of an electromagnetic wave. Radar cross sections are measured empirically, over multiple angles and frequencies.

2.6.1 Subsection Title Here

Take about an equation with text without space, like

$$\frac{1}{z}\begin{bmatrix} u \\ v \\ 1 \end{bmatrix} = K \begin{bmatrix} x \\ y \\ z \end{bmatrix} = \begin{bmatrix} f_x & 0 & c_x \\ 0 & f_y & c_y \\ 0 & 0 & 1 \end{bmatrix} \begin{bmatrix} x \\ y \\ z \end{bmatrix} \tag{4}$$

where λ can be referenced. Don't put lines before or after equations, unless the equation is the end of a paragraph's discussion.

You can also include an algorithm, like Algorithm 1.

Algorithm 1 Algorithm Title Here

function $\text{FOO}(a, b, c)$
  $\mathbf{R}_W^{C_0}, \mathbf{p}_{C_0}^W \leftarrow \text{GETPOSE}(e_0.t)$ ▷ Target pose
  for $k \leftarrow 1, N$ **do** ▷ Loop over events
    $\begin{bmatrix} x_H \\ y_H \end{bmatrix} \leftarrow \text{UNDISTPOS}(e_x, e_y)$ ▷ Pixel location to position
  end for
  return *image* ▷ Output
end function

III. Methodology

Heres what Im going to do right now:

1. Finish code to include: a. Ingest Measured object data b. Ingest sim'd object data c. Polar plots for both pols at 10GHz i. dashed lines to identify scattering centers ii. overlay plots over image iii. Overlay several rcs plots iv. plots of prob values? d. Frequency plots for both pols at i. 3D plot for freq slices f vs A vs azimuth ii. overlay sim and measurement? e. Extract probability metrics i. Amp, mean, var of each slice over frequency 2.

3.1 Calibration

Target measurements are unknown to the observer until they have been calibration. Range calibration is done by first subtracting background measurements from the target data. The corrected target data is then normalized using a ratio of simulated and measured truth data from the calibration object. The calibration object is a 7.5 inch cylinder. Additionally, background measurements are taken for both the calibration cylinder and target mounts. The formula for target calibration is shown in equation 5 [CITE].

$$\sigma_{t,true} = \frac{\sigma_{t,raw} - \sigma_{t,bg}}{\sigma_{c,raw} - \sigma_{c,bg}} \sigma_{c,true} \tag{5}$$

The raw and true measurements for the target and calibration cylinders are $\sigma_{t,raw}$, $\sigma_{t,true}$, $\sigma_{c,raw}$, and $\sigma_{c,true}$ respectively. The background measurements are taken of the target and calibration cylinders mounts, shown in the equation as $\sigma_{t,bg}$, $\sigma_{t,bg}$ respectively.

3.2 RCS Calculation

Target RCS is defined by the IEEE as shown in equation 6[12].

$$\sigma[m^2] = 4\pi \frac{|E_r|^2}{|E_r|^2} \tag{6}$$

3.3 Target Selection

This experiment is concerned with identifying the capability of a machine learning algorithm to correctly classify real radar measurements. To examine this interaction directly, targets have been chosen that produce readily measurable radar responses in a compact range. Three targets have been chosen: an oblate spheroid, a prolate spheroid, and a surrogate missile. The spheroid shapes were chosen due to their similarity, providing a classification stressor to the machine learning model. The surrogate missile has been chosen for three reasons: the nose, tail, and sides of the missile will produce 3 distinct RCS responses; the intensity of the responses for the nose, tail, and sides will be large; it is critically important for a modern military to correctly identify an ingressing missile [CITE SOMETHING FROM UKRAINE...LINK TO WHAT AIR DEFENSE DOING LOL].

Each target is modeled in Blender 3D, and exported as a .stl file. The .stl file is then imported by FreeCAD, where it is convereted to a solid and exported as a .step file. Blender allows the easy development of complex mesh shapes that do not have "holes" or "seams". FreeCAD, while have more drafting tools, does not handle mesh creation well. Object files developed in FreeCAD and imported by CADFeko were rife with mesh errors, and Altair's CADFeko program does not handle mesh repair well. This development pipeline allowed for custom model development that could easily be imported to CADFeko.

CADFeko produces a final mesh overlay for the .step file. The size and dispersement of polygons in the final overlay are driven by the simulation frequency. ”Discuss the sizing of polygons for electromagnetic simulations here, and cite something.”

The physical dimensions, electrical length, and expected RCS response for each target will be detailed in the following sections.

3.3.1 Prolate Spheroid

The prolate sphere is oblong, measuring 6 inches along its longest axis, and 3 inches at its widest. The height and width of the prolate spheroid are equivalent.

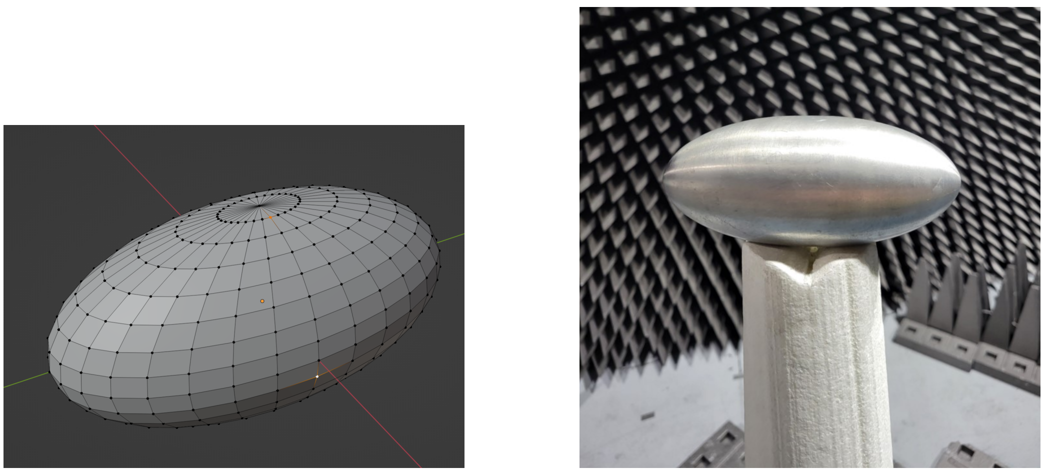

(a) Prolate sphere modeled in Blender 3D. (b) Mounted prolate sphere.

Figure 2: The simulated and physically mounted prolate sphere.

3.3.2 Oblate Spheroid

The oblate spheroid is rotationally symmteric, with a radius of 6 inches. The poles of the spheroid are 3 inches apart.

3.3.3 Missile

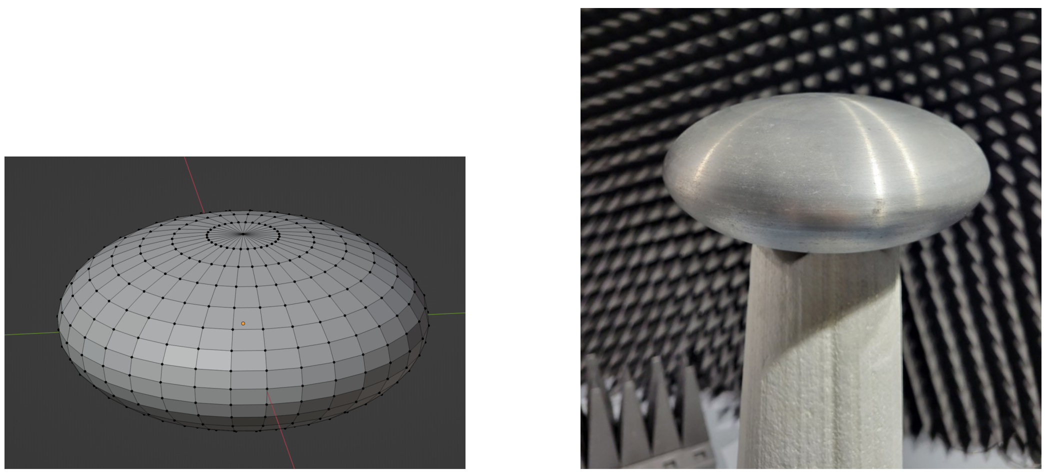

(a) Oblate sphere modeled in Blender 3D. (b) Mounted oblate sphere.

Figure 3: The simulated and physically mounted oblate sphere.

IV. Results and Analysis

4.1 Preamble

Preamble text here.

4.2 Section Title

Reference equations a little differently like (4). Or reference a table like Table 1.

Table 1: Table Title Here

Description	**Variable**	**Value**
Focal lengths	f_x	198.444
	f_y	198.826
Image Center	c_x	104.829
	c_y	92.838
Radial Distortion	k_1	-0.394
	k_2	0.156
	k_3	0
Tangential Distortion	p_1	-0.125×10^{-3}
	p_2	-1.629×10^{-3}

V. Conclusions

Conclusion text here.

5.1 Future Work

Text here

- Item 1 text here.
- Item 2 text here.

Appendix A. Additional Results

Appendix B. Second Appendix Title

Bibliography

1. R. M. Hoffer. 2020 Department of Defense Electromagnetic Spectrum Superiority Strategy. US Department of Defense `https://www.defense.gov/News/Releases/Release/Article/2397850/electromagnetic-spectrum-superiority-strategy-released/`. (Accessed: 30 August 2022).

2. E. G. Bowen. *Radar Days*. Intitute of Phsyics Publishing, 1987.

3. Scheer J. A. Holm W. A. Richards, M. A. *Noise*, pages 61–65. Scitech Publishing, Edison, NJ, 2010.

4. H. Nyquist. Thermal agitation of electric charge in conductors*. *Physical Review*, 32:110–113, 1928.

5. Scheer J. A. Holm W. A. Richards, M. A. *Noise*, pages 64–66. Scitech Publishing, Edison, NJ, 2010.

6. J. B. Johnson. Thermal agitation of electricity in conductors. *Physical Review*, 32:97–109, 1928.

7. Khalid El-Darymli, Eric W. Gill, Peter Mcguire, Desmond Power, and Cecilia Moloney. Automatic target recognition in synthetic aperture radar imagery: A state-of-the-art review. *IEEE Access*, 4:6014–6058, 2016.

8. H. S. Truman. Executive Order 10290. The American Presidency Project `https://www.presidency.ucsb.edu/node/278445`. (Accessed: 9 Sept 2022).

9. C. Campbell. China's Military: The People's Liberation Army. Congresional Research Service `https://crsreports.congress.gov/product/pdf/R/R46808`. (Accessed: 9 Sept 2022).

10. M. A. Dennis. Rodney Brooks. Britannica `https://www.britannica.com/biography/Rodney-Allen-Brooks`. (Accessed: 9 Sept 2022).

11. Creiner R. Binford T. O. Brooks, R. A. International joint conference of artificial intelligence. In *Proceesings of the International Joint Conference of Artificial Intelligence*, pages 105–113, New York, NY, 1979. ACM.

12. John Shaeffer Eugene Knott and Michael Tuley. *Radar Cross Section.* Scitech Publishing, Raleigh, NC, 2004.

Acronyms

AFIT Air Force Institute of Technology. iv

ATR Automatic Target Recognition. 2

ECM Electronic Counter Measure. iv

ESIM Electromagnetic Simulation. iv

LO Low Observable. iv

ML Machine Learning. iv

RCS Radar Cross Section. iv

ROC Radar Operating Curve. iv

SAR S. 2

REPORT DOCUMENTATION PAGE

Form Approved
OMB No. 0704–0188

1. REPORT DATE *(DD–MM–YYYY)*	2. REPORT TYPE	3. DATES COVERED *(From — To)*
19–03–2020	Master's Thesis	Sept 2018 — Mar 2020

4. TITLE AND SUBTITLE

Thesis Title
with a Second Line

5a. CONTRACT NUMBER

5b. GRANT NUMBER

5c. PROGRAM ELEMENT NUMBER

6. AUTHOR(S)

First M. Last

5d. PROJECT NUMBER

5e. TASK NUMBER

5f. WORK UNIT NUMBER

7. PERFORMING ORGANIZATION NAME(S) AND ADDRESS(ES)

Air Force Institute of Technology
Graduate School of Engineering and Management (AFIT/EN)
2950 Hobson Way
WPAFB OH 45433-7765

8. PERFORMING ORGANIZATION REPORT NUMBER

AFIT-ENG-MS-20-M-XXX

9. SPONSORING / MONITORING AGENCY NAME(S) AND ADDRESS(ES)

AFXX/XXXX
Building XXX
WPAFB OH 45433-7765
DSN XXX-XXXX, COMM 937-XXX-XXXX
Email: first.last@us.af.mil

10. SPONSOR/MONITOR'S ACRONYM(S)

XXXX/XXXX

11. SPONSOR/MONITOR'S REPORT NUMBER(S)

12. DISTRIBUTION / AVAILABILITY STATEMENT

DISTRIBUTION STATEMENT A:
APPROVED FOR PUBLIC RELEASE; DISTRIBUTION UNLIMITED.

13. SUPPLEMENTARY NOTES

14. ABSTRACT

Short abstract paragraph text here.

15. SUBJECT TERMS

subject terms here

16. SECURITY CLASSIFICATION OF: a. REPORT	b. ABSTRACT	c. THIS PAGE	17. LIMITATION OF ABSTRACT	18. NUMBER OF PAGES	19a. NAME OF RESPONSIBLE PERSON / 19b. TELEPHONE NUMBER *(include area code)*
U	U	U	UU	XXX	Captain First M. Last, AFIT/ENG (937) 255-3636, ext XXXX; first.last@afit.edu